Journal of
Computer Science & Systems Biology
ISSN: 0974-7230

Greene, J Comput Sci Syst Biol 2016, 9:5
DOI: 10.4172/jcsb.1000232

Short Communication Open Access

S2 Diode Model of Muscle Crossbridge Dynamics

Peter R Greene*

BGKT Consulting Ltd. Bioengineering, Huntington, New York, 11743, USA

Abstract

This report explores the contribution of lateral myosin bending to the developed crossbridge force and power stroke. The equipartition theorem and Boltzmann distribution are used to calculate crossbridge force and displacement, consistent with experimental values. Negligible buckling strength of the S2-myosin link means that the muscle crossbridge is effectively a one-way force transducer, a mechanical diode, transmitting axial tension forces only. Crossbridge stiffness surfaces as an important factor. Power-stroke displacement is found to decrease with increasing stiffness, whereas axial force increases. The transverse thermal fluctuations of the myosin molecule are significant. Equipartition is used to calculate the mode amplitudes for myosin bending. Crossbridge axial force Fx and power stroke Δx develop from transverse in-plane fluctuations along the y and z axes. Single and double-headed actin-myosin attachment configurations are calculated in detail. Practical applications include the effects of temperature on the flexibility of the myosin molecule stiffness and tension, relevant to man-made fabrication of synthetic muscle using micro-machines. Scaling laws for the S2 bending amplitude depend on mode number, filament length, and stiffness, as $(n)^{-2}$, $(L)^2$, and $(EI)^{-1}$.

Keywords: Actin-myosin; Muscle crossbridge; Axial force; Brownian motion; Stiffness; Scaling laws

Introduction

The muscle crossbridge structure is a highly efficient molecular machine. An understanding of the dynamics of crossbridge conformational changes are central to our understanding of the mechanism of chemo-mechanical transduction by motor proteins. The purpose of this report is to investigate the molecular dynamics of the skeletal muscle crossbridge, in particular, the contribution of thermal fluctuations of the S1 and S2 components of myosin. Basically an articulated molecule, as shown in Figure 1a, the myosin S1 segment is usually modelled as a 2, 3, or 4 position ratchet, similar to the escapement mechanism on a mechanical pendulum clock, generating force by rocking forward, as shown.

Reviews

Theories are many and varied in terms of explaining how the crossbridge generates axial force. Cooke [1] reviews various theoretical models for muscle crossbridge mechanics. Nie et al. [2] analyze the effect of Brownian motion on force generation in the muscle crossbridge. Greene [3-5] calculates thermal fluctuation effects on force generation and stiffness, finding values of 2×10^{-12} to 5×10^{-12} N/XB. Muscle physiology and crossbridge dynamics are reviewed by Cooke [1], McMahon [6], Carlson and Wilke [7], and McMahon and Greene [8].

Flexibility

Gittes et al. [9] measure the flexibility of actin filaments by analyzing the thermal fluctuations in shape. Yoshimura et al. [10] measure torsional flexibility of F-Actin. Kishino and Yanagida [11] measure the force required to stretch F-actin filaments. Nagashima and Asakura [12] measure the end-to-end length changes of F-actin due to thermal fluctuations. Liu [13] measure the distribution of S1-S2 flexible angles concluding that both positive and negative crossbridge forces are found in the rigor state. Using fast freezing, Liu et al. [14] measure S1 strain displacements as large as 45 A˚ in stretched rigor fibers. Davis and Harrington [15] report temperature effects on muscle force generation and stiffness, relevant to the thermodynamics of the S2 chain, suggesting that the S1 segment rocks backwards during the powerstroke.

Tension and compression

Adamovic et al. [16] measure directly the stretching and flexible bending stiffness of the LMM domain of myosin from scallop, finding values of 60-80 pN/nm and 0.010 pN/nm respectively, i.e., relatively compliant in bending. Kaya and Higuchi [17] using optical techniques measure directly the compression and tension characteristics of myosin, finding a small buckling load when strained negatively, with a working power stroke of 80 A˚. Finer, Simmons and Spudich [18] measure a working step length of 110 A˚ and axial force per crossbridge of 3-4 pN. Dobbie et al. [19] measure the contribution of the S1 myosin head region to crossbridge compliance, using X-ray diffraction finding displacements of 20-27 A˚. Stewart McLachlan and Calladine [20] model the S2 portion of myosin, finding axial displacements of 30-40 A˚. Seo, Krause and McMahon measure S2 buckling characteristics [21] in muscle fibers during quick release tension experiments.

Computer calculations

Huxley [22] reviews the mechanics of the muscle crossbridge. Slawnych, Seow, Huxley and Ford [23] develop a computer program to predict crossbridge performance. Billington et al. [24] report the thermal effects on lever-arm flexibility of the S1-S2 junction, with values of 0.37 pN/nm stiffness. Golji et al. [25] model the molecular dynamics of α-Actinin (similar to but larger than F-actin) applying bending forces in the range 8 to 200 pN and torques of 50-500 pN-nm over a rapid time scale of 10 to 100 picosecs. Pang [26] performs molecular dynamics calculations on a time scale of femtosecs.

***Corresponding author:** Peter R Greene, BGKT Consulting Ltd. Bioengineering, Huntington, New York, 11743, USA, Tel: +16319355666; E-mail: prgreeneBGKT@gmail.com

Received April 25, 2016; **Accepted** September 06, 2016; **Published** September 15, 2016

Citation: Greene PR (2016) S2 Diode Model of Muscle Crossbridge Dynamics. J Comput Sci Syst Biol 9: 150-153. doi:10.4172/jcsb.1000232

Copyright: © 2016 Greene PR. This is an open-access article distributed under the terms of the Creative Commons Attribution License, which permits unrestricted use, distribution, and reproduction in any medium, provided the original author and source are credited.

Materials and Methods

Basic equations for bending and buckling of the myosin rod include actin F1 and myosin S2 bending and buckling, S2 mode amplitudes, and equipartition energy per mode [6]. As shown in Figure 1a, the x-axis is parallel to the developed force, the y-axis is vertical, and the z-axis is perpendicular to the xy-plane. Axial force Fx and power stroke Δx is produced by transverse in-plane fluctuations of S2 along the y and z axes. The origin of the coordinate system is at the S1-S2 junction. Myosin S2 buckling load is assumed minimal, Figure 1b, as measured [10a, 10b, 17a].

In-plane Δy and out-of-plane Δz fluctuations are independent of each other. The individual contributions are found by calculating the r.m.s. average,

$$\Delta x = \text{sqr}\,[\Delta xy^2 + \Delta xz^2] \quad (1)$$

Developed axial force results from integrating the Boltzmann distribution with the S1 spring stiffness in tension,

$$Fx = Co \int (Kx)\exp(-0.5\,Kx^2 / kT)\,dx \qquad 0<x<\infty \quad (2)$$

where axial force F=Kx in tension for x>0, and F=0 for x<0 in compression, Figure 1b. The F-actin thin filament is also flexible in torsional mode [3]. The amplitudes Θn are found to scale as n^{-1}, $(EI)^{-1/2}$, and $L^{1/2}$, where n is mode number, EI is actin bending stiffness, and L is filament length. Depending on conditions, the twisting modes can be as large as +/- 150. Similar scaling laws are found here for S2 bending, Table 1, showing scaling laws for S2 amplitude depends on filament length, mode number, and stiffness, Table 1.

Results

Harmonic mode amplitude for the over-tone sequence scales as $(\#n)^{-2}$, $(L)^2$, and $(EI)^{-1}$ (Table 1; Figures 1 and 2). Power stroke for mode #n scales as

$$\Delta x/Lo = 2.5\,(An / L)^2 \quad (3)$$

The first 3 principle modes (n=1, 2, 3) are shown in Figure 2 below, A1=+/-100 A˚. Figure 3a shows the equipartition distribution of S1 axial position about its equilibrium point, calculated from Eq. (4) 0.5 kT=0.5 K $\langle x^2 \rangle$. Figures 3b, 3c and 3d show force and displacement for the single and doubly-attached S1 myosin head depends strongly on crossbridge stiffness.

Crossbridge force is estimated at Fx_y=1.0 pN for the in-plane component, Fx_{yz}=1.4 pN for both in-plane and out-of-plane combined. Crossbridge power-stroke is estimated at dxy=40 A˚ for the in-plane component, dx_{yz}=56 A˚ for both the Δy and Δz fluctuations included. Minimal assumptions include [1] S2 link is inextensible with minimal buckling load and [2] experimental crossbridge compliance K is given by Eq. 4:

$$dF/dx = 4 \times 10^{-4}\ \text{N/m},\ K = 8 \times 10^{-4}\ \text{N/m}\ \text{for S1 double-head configuration} \quad (4)$$

It is provided by S1 (Huxley and Simmons [27]). Muller et al. [28] calculate flexural details of the S2 link. An IBM PC-XT was used for the calculations, running MicroSoft Basic 3.2 at 4.77 MHz, then re-confirmed with an online Windows compatible version of QBasic, running at 500-1,000 MHz, distributed by JustBasic.com [29]. Original calculations were made on an Apple II Computer running at 1 MHz. Modern computers, now 1,000 times faster, can perform the integrations in Eq. 2 in just 1-second, whereas previously 15-20 minutes were required.

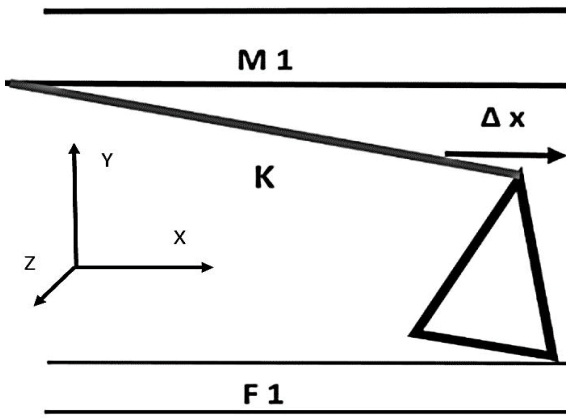

Figure 1a: Crossbridge schematic shows thin filament F1, thick filament M1, and x-y-z coordinate system.

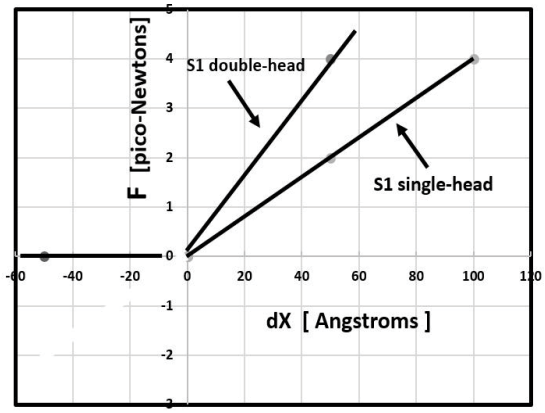

Figure 1b: Diode tension characteristic curves for myosin S1 single-head, stiffness K=4 × 10^{-4} N/m, and S1 double-head configurations, K=8 × 10^{-4} N/m.

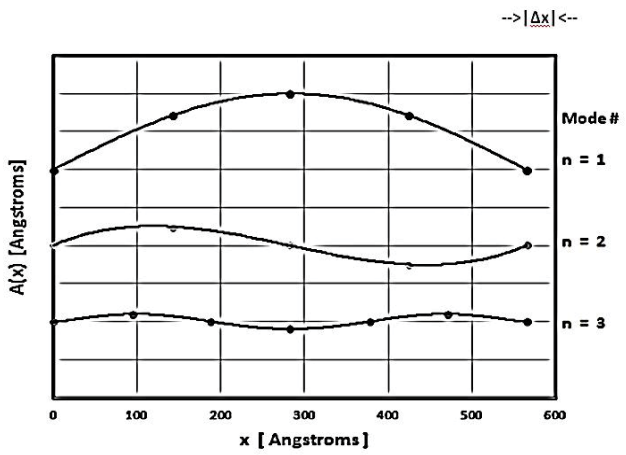

Figure 2: Myosin rod harmonic bending modes for n=1, 2, 3, drawn to scale.

Mode	# n	Length (L)	Stiffness (EI)
Torsion	n^{-1}	$L^{1/2}$	$(EI)^{-1/2}$
Tension	n^{-2}	L^2	$(EI)^{-1}$

Table 1: Scaling Effects for Thermal Oscillation Amplitude.

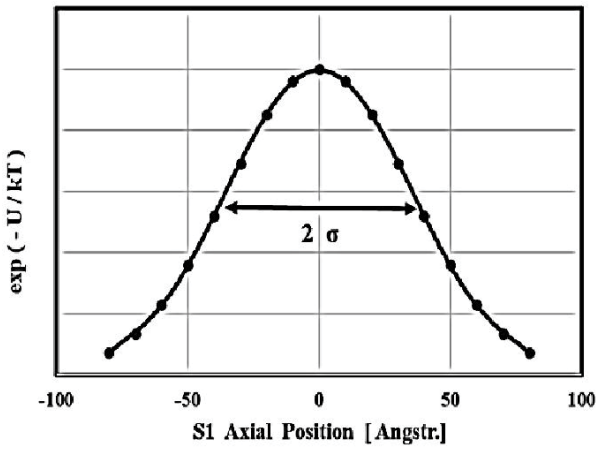

Figure 3a: Boltzmann distrib., S1 position, σ=+/-32 A°.

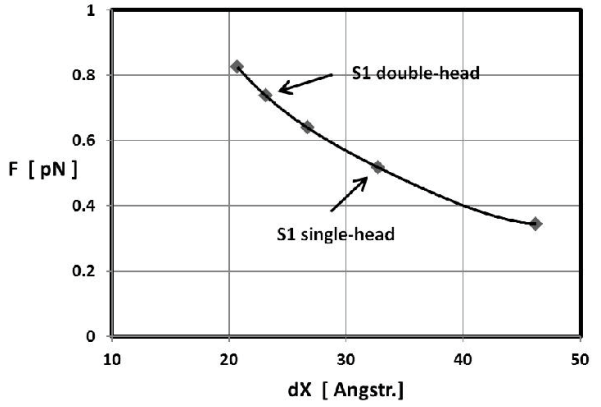

Figure 3b: Crossbridge force F [pN] vs. dX [A°].

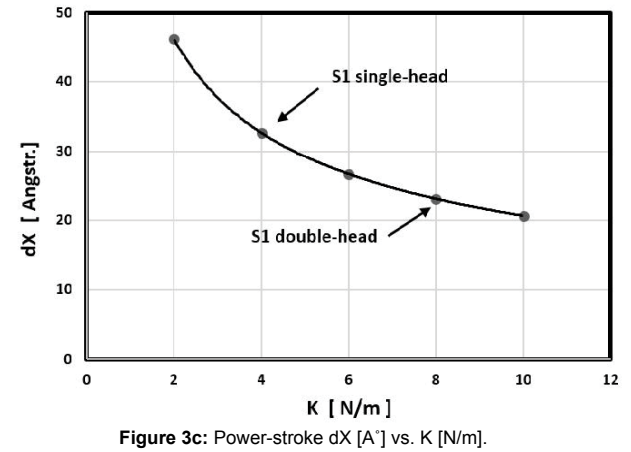

Figure 3c: Power-stroke dX [A°] vs. K [N/m].

Interestingly, the n=2 harmonic mode is particularly efficient at generating a power stroke, because the axial shortening of S2 scales as ~ n^2, approximately 30 A° power stroke for a lateral mode amplitude of 25 A°. This is important because the available steric space varies with inter-filament spacing. This n^2 effect offsets the mode amplitude reduction, which scales as n^{-2}. In addition to evaluating the arc-length integral, given by Eq. 5:

$$\int \mathrm{sqr}[(dx)^2+(dy)^2]=Lo \qquad 0<x<L \tag{5}$$

The length reduction was confirmed with a 12" spline (Dietzgen Corp.).

Discussion

Spider-Web monofilament model

Results presented here do not only apply to microscopic systems. For instance, a spider web stretched between two trees over a distance of 6 to 10 feet (2 to 3 meters) will fluctuate in the wind. The author has observed the n=1, 2, and 3 modes of these mono-filaments, buffeted by eddies in the wind on a still day, and the resulting bending of the leaf to which the filament is attached. This experimental observation, demonstrating the "clothesline effect", may be important, as it represents the limiting case of zero bending stiffness, similar to the S2 segment of myosin. In other words, amplified axial force is developed by transverse flexing of the S2 filament.

Doubly attached myosin S1 head

The purpose of the second myosin (Figure 1a) head is still unknown [29-31]. Under some circumstances, both heads can co-attach, either to the same actin filament, or adjacent actin filaments, which effectively doubles the stiffness of the bridge, Figures 1b, 3b, 3c and 3d. From a thermodynamic point of view, the second head represents another ½ kT degree of freedom of the system. AC Power cable comparison. While power from random motion seems counter-intuitive, a familiar example serves to illustrate: fluctuating (+) and (-) voltages, after passing through a diode bridge, result in an average net (+) positive voltage. Likewise, AC power cables, in a wind-driven turbulent velocity field, result only in (+) positive cable tension, because cables cannot sustain buckling force in compression. Results presented here are a uni-directional tension-only mechanical model, hence the name "Myosin Diode Model", because only positive forces can be transmitted through the S2-linkage.

Equipartition energy

The thermal fluctuations of the S1 motor head alone result in fractional pico-Newton forces on the S2 myosin and the actin filaments, considerably "under-powered" compared with the experimentally observed force per crossbridge. These force and displacement values correspond to ~ 0.5 kT of thermal energy and are comparable to the natural thermal fluctuations of the system. Note that the additional degrees of freedom of the S2 segment result in additional axial force from each independently oscillating mode, summed as per Eq. 1.

Applications

Results presented here show that during transverse thermal fluctuations of the myosin molecule, a significant axial crossbridge force and power stroke is developed from random transverse thermal motion (Figures 3b-3d). Practical applications include the effects of temperature on the flexibility of the myosin molecule [32,33]. Man-made fabrication of muscle is now possible, using micro-machines, so it is of interest to specify the role of Brownian motion on the mechanics of miniature molecular motors similar to the crossbridge [34,35]. In terms of the bioengineering design of these synthetic muscles, design objectives include determining the optimum length filament (equivalent to myosin), optimum stiffness, harmonic mode number, and optimum inter- filament spacing, for maximum crossbridge force, power stroke, and thermodynamic efficiency.

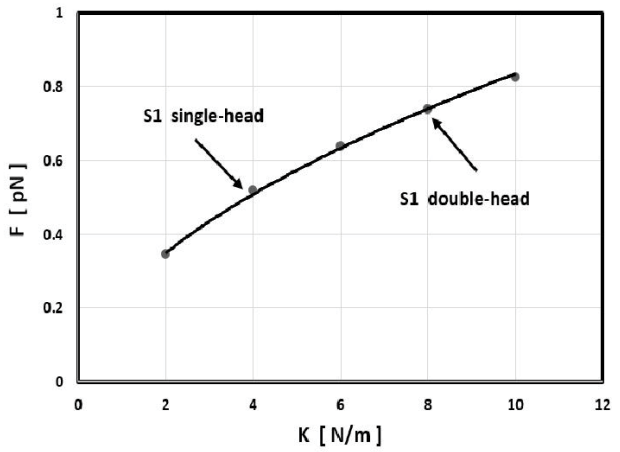

Figure 3d: Force F [pN] vs. stiffness K [N/m].

Acknowledgements

This work was funded in part by a Whitaker Foundation Bioengineering Grant at The Johns Hopkins University, Department of Biomedical Engineering.

Nomenclature

Δx=Crossbridge power stroke=40 to 100 A°

K=Crossbridge stiffness=4 × 10^{-4} N/m to 8 × 10^{-4} N/m (chevron)

F/XB=2 to 4 × 10^{-12} N/XB=2 pN to 4 pN

Lo=resting length of myosin=600 A°

0.5 kT=Equipartition energy, k=1.38 × 10^{-16} ergs/K^0=1.38 × 10^{-23} J/ K^0

exp(-U/kT)=Boltzmann factor, U=0.5 K × 2 elastic energy

Co=∫ exp(-0.5 Kx^2/kT)dx, Boltzmann constant

References

1. Cooke R (2004) The sliding filament model: 1972-2004. J Gen Physiol 123: 643-656.
2. Nie QM, Togashi A, Sasaki TN, Takano M, Sasai M, et al. (2014) Coupling of lever arm swing and biased Brownian motion in actomyosin. PLoS Comput Biol. 10: e1003552.
3. Greene PR (1985) Thermal torsion of F-actin. J Theor Biol. 117: 489-492.
4. Greene PR, McMahon TA (1979) Reflex stiffness of man's anti-gravity muscles during kneebends while carrying extra weights. J Biomech. 12: 881-891.
5. Greene PR (1983) Axial Force from Transverse Motions of the Crossbridge. Biophys J 41: 146a.
6. McMahon TA (1984) Muscle Reflexes and Locomotion. Princeton University Press, NJ, USA, p: 354.
7. Carlson FD, Wilkie DR (1974) Muscle physiology. Prentice-Hall Inc., USA.
8. McMahon TA, Greene PR (1978) Fast running tracks. Sci Am. 239: 148-163.
9. Gittes F, Mickey B, Nettleton J, Howard J (1993) Flexural rigidity of microtubules and actin filaments measured from thermal fluctuations in shape. J Cell Biol. 120: 923-934.
10. Yoshimura H, Nishio T, Mihashi K, Kinosita K Jr, Ikegami A (1984) Torsional motion of eosin-labeled F-actin as detected in the time-resolved anisotropy decay of the probe in the sub-millisecond time range. J Mol Biol 179: 453-467.
11. Kishino A, Yanagida T (1988) Force measurements by micromanipulation of a single actin filament by glass needles. Nature 334: 74-76.
12. Nagashima H, Asakura S (1980) Dark-field light microscopic study of the flexibility of F-actin complexes. J Mol Biol. 136: 169-182.
13. Liu J, Wu S, Reedy MC, Winkler H, Lucaveche C, et al. (2006) Electron tomography of swollen rigor fibers of insect flight muscle reveals a short and variably angled S2 domain. J Mol Biol. 362: 844-860.
14. Liu J, Reedy MC, Goldman YE, Franzini-Armstrong C, Sasaki H, et al. (2004) Electron tomography of fast frozen, stretched rigor fibers reveals elastic distortions in the myosin crossbridges. J Struct Biol. 147: 268-282.
15. Davis JS, Harrington WF (1993) A single order-disorder transition generates tension during the Huxley-Simmons phase 2 in muscle. Biophys J. 65: 1886-1898.
16. Adamovic I, Mijailovich SM, Karplus M (2008) The elastic properties of the structurally characterized myosin II S2 subdomain: a molecular dynamics and normal mode analysis. Biophys J. 94: 3779-3789.
17. Kaya M, Higuchi H (2010) Nonlinear elasticity and an 8-nm working stroke of single myosin molecules in 28 myofilaments. 329: 686-689.
18. Finer JT, Simmons RM, Spudich JA (1994) Single myosin molecule mechanics: piconewton forces and nanometre steps. Nature 368: 113-119.
19. Dobbie I, Linari M, Piazzesi G, Reconditi M, Koubassova N, et al. (1998) Elastic bending and active tilting of myosin heads during muscle contraction. Nature 396: 383-387.
20. Stewart M, McLachlan AD, Calladine CR (1987) A model to account for the elastic element in muscle crossbridges in terms of a bending myosin rod. Proc R Soc Lond B Biol Sci. 229: 381-413.
21. Seo JS, Krause PC, McMahon TA (1994) Negative developed tension in rapidly shortening whole frog muscles. J Muscle Res Cell Motil. 15: 59-68.
22. Huxley AF (2000) Mechanics and models of the myosin motor. Philos Trans R Soc Lond B Biol Sci. 355: 433-440.
23. Slawnych MP, Seow CY, Huxley AF, Ford LE (1994) A program for developing a comprehensive mathematical description of the crossbridge cycle of muscle. Biophys J. 67: 1669-1677.
24. Billington N, Revill DJ, Burgess SA, Chantler PD, Knight PJ (2014) Flexibility within the heads of muscle myosin-2 molecules. J Mol Biol. 426: 894-907.
25. Golji J, Collins R, Mofrad MR (2009) Molecular mechanics of the alpha-actinin rod domain: bending, torsional, and extensional behavior. PLoS Comput Biol. 5: e1000389.
26. Pang YP (2014) Low-mass molecular dynamics simulation: a simple and generic technique to enhance configurational sampling. Biochem Biophys Res Commun. 452: 588-592.
27. Huxley AF, Simmons RM (1971) Proposed mechanism of force generation in striated muscle. Nature 233: 533-538.
28. Müller KW, Birzle AM, Wall WA (2016) Beam finite-element model of a molecular motor for the simulation of active fibre networks. Proc Math Phys Eng Sci. 472: 20150555.
29. Greene PR (In Press) Effects of Thermal Tension Transients on the Muscle Crossbridge. BRL.
30. Tozeren A (1987) The influence of doubly attached crossbridges on the mechanical behavior of skeletal muscle fibers under equilibrium conditions. Biophys J. 52: 901-906.
31. Tözeren A, Schoenberg M (1986) The effect of cross-bridge clustering and head-head competition on the mechanical response of skeletal muscle under equilibrium conditions. Biophys J. 50: 875-884.
32. Woledge RC, Barclay CJ, Curtin NA (2009) Temperature change as a probe of muscle crossbridge kinetics: a review and discussion. Proc Biol Sci. 276: 2685-2695.
33. Dickinson M, Farman G, Frye M, Bekyarova T, Gore D, et al. (2005) Molecular dynamics of cyclically contracting insect flight muscle in vivo. Nature 433: 330-334.
34. Kinosita K Jr, Yasuda R, Noji H, Adachi K (2000) A rotary molecular motor that can work at near 100% efficiency. Philos Trans R Soc Lond B Biol Sci. 355: 473-489.
35. Lard M, ten Siethoff L, Generosi J, Persson M, Linke H, et al. (2015) Nanowire-imposed geometrical control in studies of actomyosin motor function. IEEE Trans Nanobioscience 14: 289-297.